The Henryk Niewodniczański
INSTITUTE OF NUCLEAR PHYSICS
Polish Academy of Sciences
ul. Radzikowskiego 152, 31-342 Kraków, Poland

Kraków, January 2017

Report No. 2098/AP

Calculations of the neutron-induced activity in air inside the Cuboid 2 of the High-Resolution Neutron Spectrometer for ITER

Anna Wójcik-Gargula, Grzegorz Tracz, *Marek Scholz, Krzysztof Drozdowicz*

Institute of Nuclear Physics PAN, Radzikowskiego 152, 31-342 Kraków, Poland

This work has received funding from Fusion for Energy (F4E) research program under grant agreement No F4E-GRT-403 (DG)**.** The views and opinions expressed herein do not necessarily reflect those of the European Commission.

Abstract

This report presents results of the calculations performed in order to predict the neutron-induced activity in air inside the second Cuboid in the ITER equatorial port cell #1 where the Time of Flight detectors of the High Resolution Neutron Spectrometer are planned to be installed. Based on the neutron spectra generated by 2.45 MeV and 14 MeV neutron sources, calculated with the MCNP code, it was possible to determine the activity of the dominant radionuclides using the FISPACT-II Transmutation - Activation Inventory Code and the EAF-2010 nuclear data library. The results show that although long-lived isotopes such as e.g. H-3 or C-14 are produced following neutron irradiation, their activity will not be significant since they will not exceed the maximum permissible levels.

Introduction

The High Resolution Neutron Spectrometer (HRNS) is a part of the ITER neutron diagnostics system allowing the determination of the core plasma fuel ratio (i.e. the amount of tritium and deuterium

(n_T/n_D) in the plasma) as well as the provision of information on the ion temperature profile [1]. Although the concept for this diagnostics is still in the course of design, at the beginning of the ITER design phase a decision has been made that HRNS will be installed by adding a collimator into the radial neutron camera (RNC) located in the ITER equatorial port #1. Then, HRNS would be installed behind RNC, the bioshield and the radial gamma-ray spectrometer (RGRS) (Fig.1) [2] and it would be using the central line of sight (LoS) of RNC (Fig.2) [3]. The recently developed concept of HRNS for ITER assumes the use of the following set of detection systems (Fig.3)[4]:

- TPR -- Thin-foil Proton Recoil Spectrometer,
- Diamond detectors[1],
- ToF - Time-Of-Flight (TOF) neutron spectrometer Optimized (O) for high count Rate (R) measurements of neutrons from fusion reactions,
- b-TOF -- TOF back-scattering spectrometer.

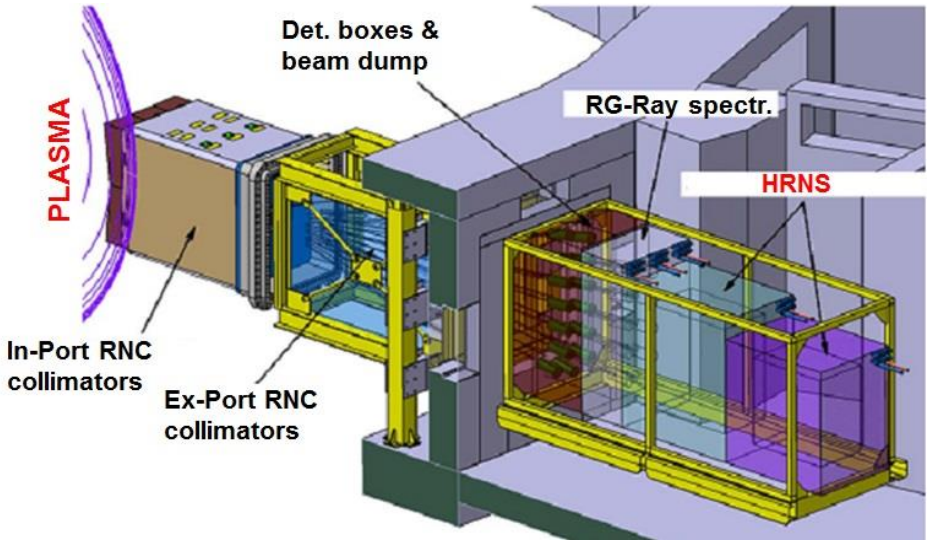

Fig.1. Location of HRNS and other diagnostics (i.e. RNC and RGRS) in the ITER equatorial port #1 [2].

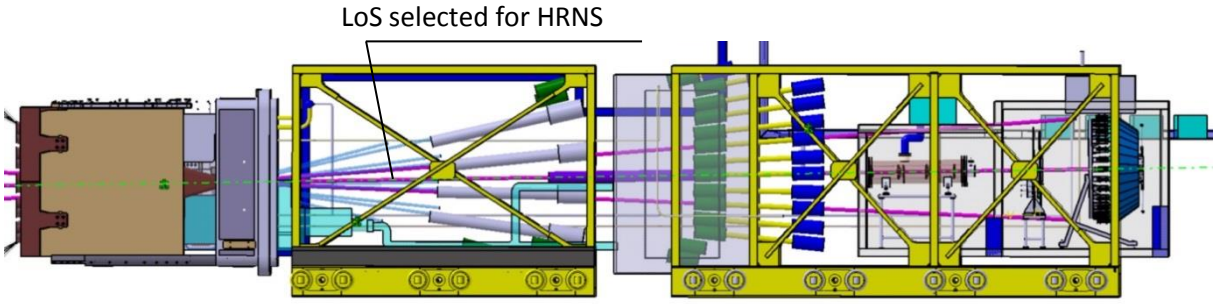

Fig.2. LoS (line of sight) selected for HRNS [3].

[1] in Fig.3. marked as NDD

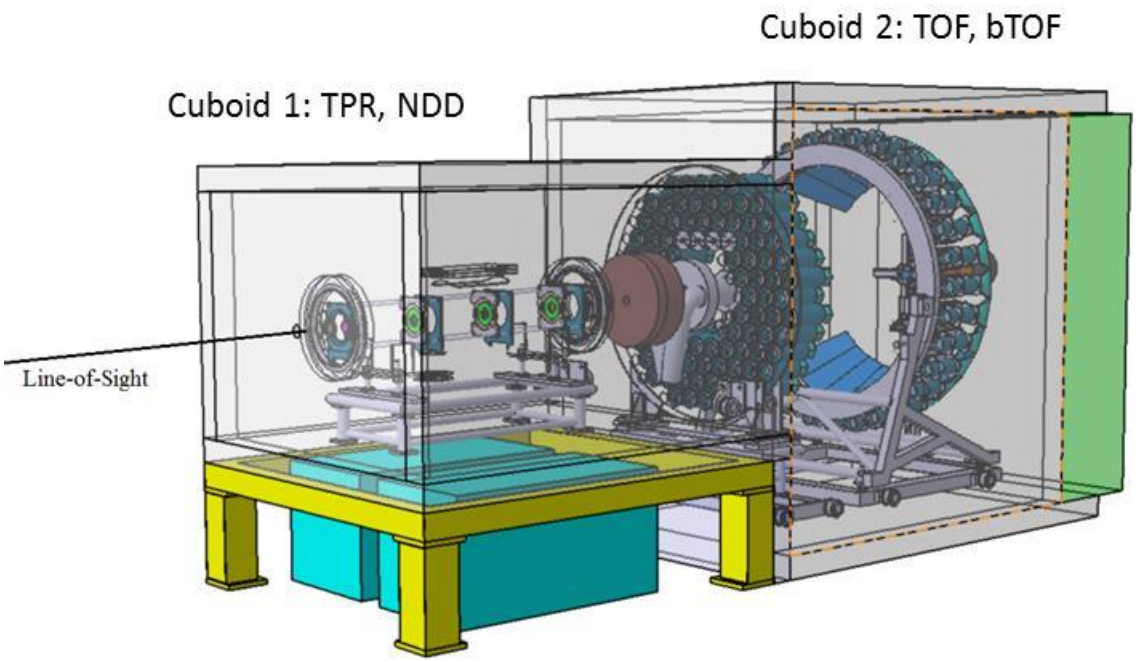

Fig.3. Arrangement of the HRNS system in the ITER equatorial port cell #1 [4].

These detectors comprise two joined sub-systems located in so called Cuboids in the ITER port cell #1: a TPR spectrometer and diamond detectors in the first Cuboid, ToF detectors in the second Cuboid. The ToF detectors consist of around 180 photomultiplier tubes (PMTs). These PMTs are supplied with a high voltage (≤ 2kV) and the resulting currents are ≤ 1 mA which gives a total power consumption of around 350 W. Since, the PMTs temperature has to be stabilized to the level of 22°C +/- 2°C, the air-cooling system with individual nozzles for each detector of ToF and bTOF has been proposed. However, a question arose how much the neutron flux reaching the second cuboid activates the air inside it. This report presents the results of the calculations performed in order to predict the neutron-induced activity in air inside the Cuboid 2 in the ITER port cell #1.

MCNP and FISPACT calculations

Neutronic calculations were performed using the MCNP5 code [5] to provide the neutron spectra in the Cuboid 2 generated by 2.45 MeV and 14 MeV neutron sources. Fig. 4 presents these spectra in the Vitamin-J 175 energy group structure. The neutron spectra in the entire volume of the second cuboid were calculated. Each Monte Carlo simulation was carried out for 10^9 histories. The error on the flux in each energy bin was typically around 0.1%.

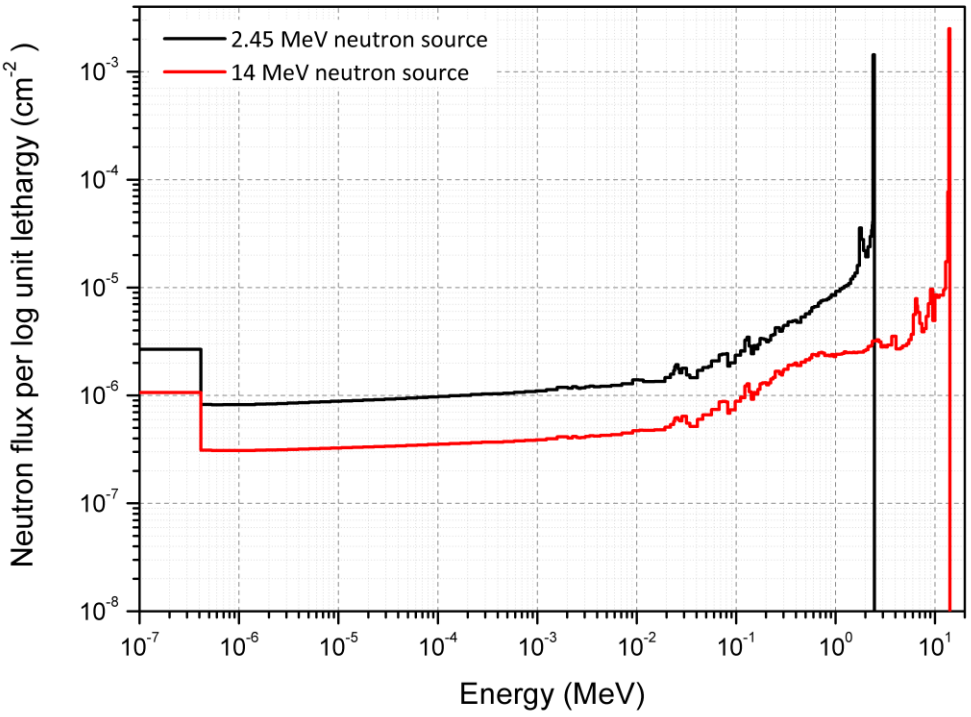

Fig.4. Neutron spectra in cuboid 2 generated by 2.45 MeV and 14 MeV neutron sources, calculated using the MCNP5 code. Fluxes are normalized per one source neutron.

Table 1 presents the gaseous composition of dry air at ground level in remote continental areas [6]. The considered cuboid has the volume (V) of 4.80 m^3 (dimensions: 205 cm x 130 cm x 180 cm). The density of air at the temperature T= 295.15 K and at the sea level standard atmospheric pressure of 101325 Pa is equal to 1.20 $kg \cdot m^{-3}$. Thus, the mass of air in the cuboid m = 5.74 kg.

Table 1. Gaseous composition of dry air [6]

Constituent	%	ppm
N_2	78.084	780 840
O_2	20.946	209 460
Ar	0.934	9340
CO_2	0.0360	360
Ne	0.00181	18.18
He	0.00052	5.24
CH_4	0.00017	1.70
Kr	0.00011	1.14
H_2	0.00005	0.50
Xe	0.000008	0.087

The neutron flux entering the Cuboid 2 was calculated by using the following formula [4]:

$$F_n = \frac{A_A L_I}{4\pi C_L^2},$$

where:

$-\ A_A$ - area of the aperture in the ITER first wall,

$-\ L_I$ - line integral, corresponding to the neutron emissivity integral along the center of the LoS,

$-\ C_L$ - distance from the first wall to the Cuboid 2.

At a fusion power of 500 MW: $F_n = 7.93{\cdot}10^{12}$ n·m^{-2}·s^{-1}. Taking into account the diameter of the radial LoS equal to 10 cm and a standard ITER discharge duration of 400 s, one can obtain a total neutron budget in the Cuboid 2 on the level of $2.49{\cdot}10^{13}$ neutrons (for one ITER shot). In the calculations of the neutron-induced activity the irradiation scenario based on the so called 'safety operating scenario' (designated as SA2) [7] was considered. In this scenario, two years of DD plasma operation, with a total neutron fluence of 0.006 MW·yr·m^{-2}, are foreseen. At a fusion power of 2.68 MW the total neutron fluence and the mean neutron flux in the Cuboid 2 for 2.45 MeV neutron source were calculated to be $6.70{\cdot}10^{6}$ n·cm^{-2} and $1.68{\cdot}10^{6}$ n·cm^{-2}·s^{-1}, respectively. The total neutron fluence and the mean neutron flux in the Cuboid 2 for 14 MeV neutron source (DT plasma operation) and the fusion power of 500 MW were equal to $1.04{\cdot}10^{9}$ n·cm^{-2} and $2.59{\cdot}10^{9}$n·cm^{-2}·s^{-1}, respectively.

Eventually, the composition of dry air and the calculated neutron spectra and mean neutron fluxes were used as input parameters to the FISPACT-II Transmutation-Activation Inventory Code [8]. The simulations of the evolution in activation and the transmutation (burn-up) of radionuclides in air under neutron irradiation were performed using the EAF-2010 nuclear data libraries[2] compiled specifically for fusion-relevant calculations with FISPACT.

Additionally, it was assumed that no ventilation flow is present in the Cuboid.

The activities of the dominant radionuclides a) per 1 gram of air (specific activities) and b) for a total mass of air in the Cuboid m = 5.74 kg were calculated for two discharge durations: 400 s (a standard burn duration in inductive ITER operation) and for 3000 s (typical burn duration in non-inductive operation) [9]. For all the considered cases, the activity levels were determined at several different times after the end of irradiation (a.o. at 1 min, 10 min, 1 h, 10 h, 24 h).

Results of the FISPACT-II calculations

In the case of the 2.45 MeV neutron source, the dominant isotopes produced due to the activation of air inside the Cuboid 2 are Ar-41 ($T_{1/2}$ = 1.82 h), Ar-37 ($T_{1/2}$ = 35.04 d) and C-14 ($T_{1/2}$ = 5730 y). Table 2 and Fig. 5 & 6 show the calculated activities of the dominant radionuclides in air 0-24 hours after the end of irradiation (EOI) lasting 400 s and 3000s, respectively. The total activity of air inside the Cuboid 2 after the irradiation lasting 400 or 3000 s was found to be rather low e.g. (7.96E+01 ± 3.23E-02)Bq and (5.00E+02 ± 4.53E-03)Bq at 1 min after the end of irradiation (EOI); (6.49E-03 ± 3.22E-04)Bq and (4.87E-02 ± 4.44E-03)Bq at 24 h after EOI. Ar-41 gives a major contribution to the total activity of air up to about 15 hours after EOI. Over this period of time this contribution reaches

[2] See the Appendix 1 for further details.

~99.9%. Ar-41 is produced via (n,γ) reaction on Ar-40. It decays to K-41 emitting a beta- particle with a maximum energy of 1.2MeV and a photon of 1.29 MeV (yield 99.2%), or a beta- of 2.485 MeV (yield 0.78%). During the considered time period (24 hours), the activities of long lived radionuclides - i.e. Ar-37 and C-14 - remain on the level of hundredth (Ar-37) or thousandth parts of Bq (C-14).

Table 2. Activities of dominant radionuclides in air 0-24 hours after the end of irradiation lasting 400 s and 3000s (2.45 MeV neutron source; fusion power: 2.68 MW; air mass m=5.74 kg).

	t = 1 min		***t = 10 min***		***t = 1 h***	
Nuclide	**A(t_{irr}=400s) [Bq]**	**A(t_{irr}=3000s) [Bq]**	**A(t_{irr}=400s) [Bq]**	**A(t_{irr}=3000s) [Bq]**	**A(t_{irr}=400s) [Bq]**	**A(t_{irr}=3000s) [Bq]**
Ar-41	7.96E+01	5.00E+02	7.53E+01	4.73E+02	5.53E+01	3.45E+02
Ar-37	4.58E-03	3.44E-02	4.58E-03	3.44E-02	4.58E-03	3.43E-02
C-14	2.00E-03	1.50E-02	2.00E-03	1.50E-02	2.00E-03	1.50E-02
A_{total}=	7.96E+01	5.00E+02	7.53E+01	4.73E+02	5.53E+01	3.45E+02
	t = 5 h		***t = 10 h***		***t = 24 h***	
Nuclide	**A(t_{irr}=400s) [Bq]**	**A(t_{irr}=3000s) [Bq]**	**A(t_{irr}=400s) [Bq]**	**A(t_{irr}=3000s) [Bq]**	**A(t_{irr}=400s) [Bq]**	**A(t_{irr}=3000s) [Bq]**
Ar-41	1.53E+01	7.80E+02	4.20E+00	8.86E+00		
Ar-37	4.56E-03	3.42E-02	4.55E-03	3.41E-02	4.49E-03	3.37E-02
C-14	2.00E-03	1.50E-02	2.00E-03	1.50E-02	2.00E-03	1.50E-02
A_{total}=	1.53E+01	7.81E+02	4.20E+00	8.91E+00	6.49E-03	4.87E-02

A_{total} – total activity [Bq]; t_{irr} – time of irradiation (duration of a discharge)

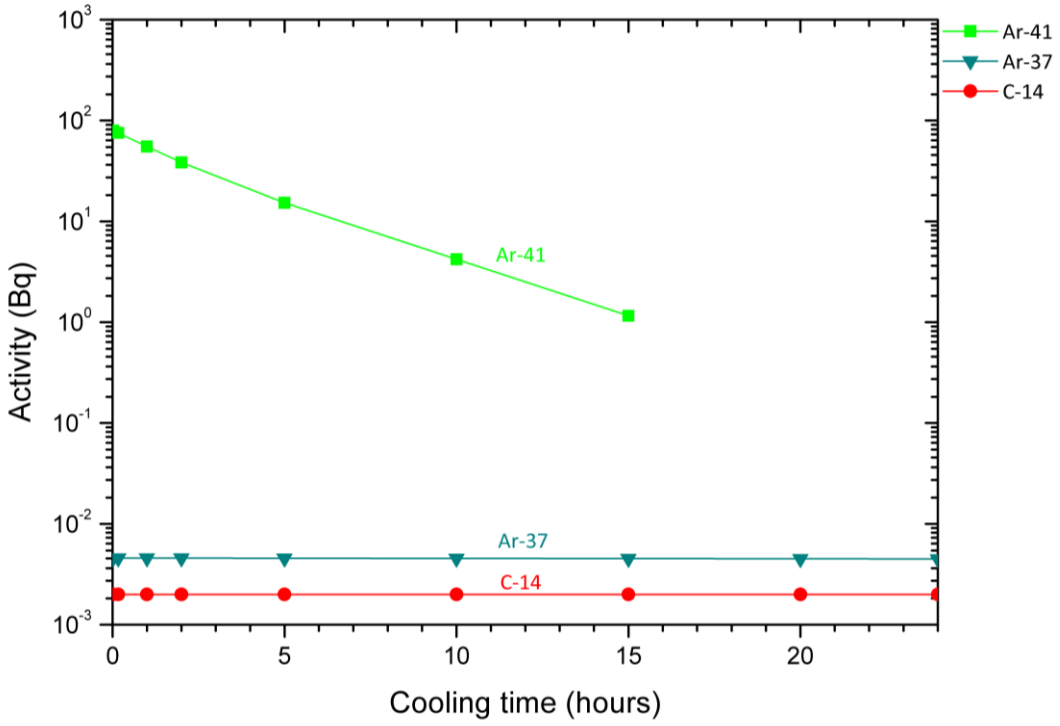

Fig.5. Activity of dominant radionuclides in air 0-24 hours after the end of activation with 2.45 MeV neutron source (fusion power: 2.68 MW; time of irradiation: 400 s). Data shown only when the number of atoms is greater than $1 \cdot 10^4$.

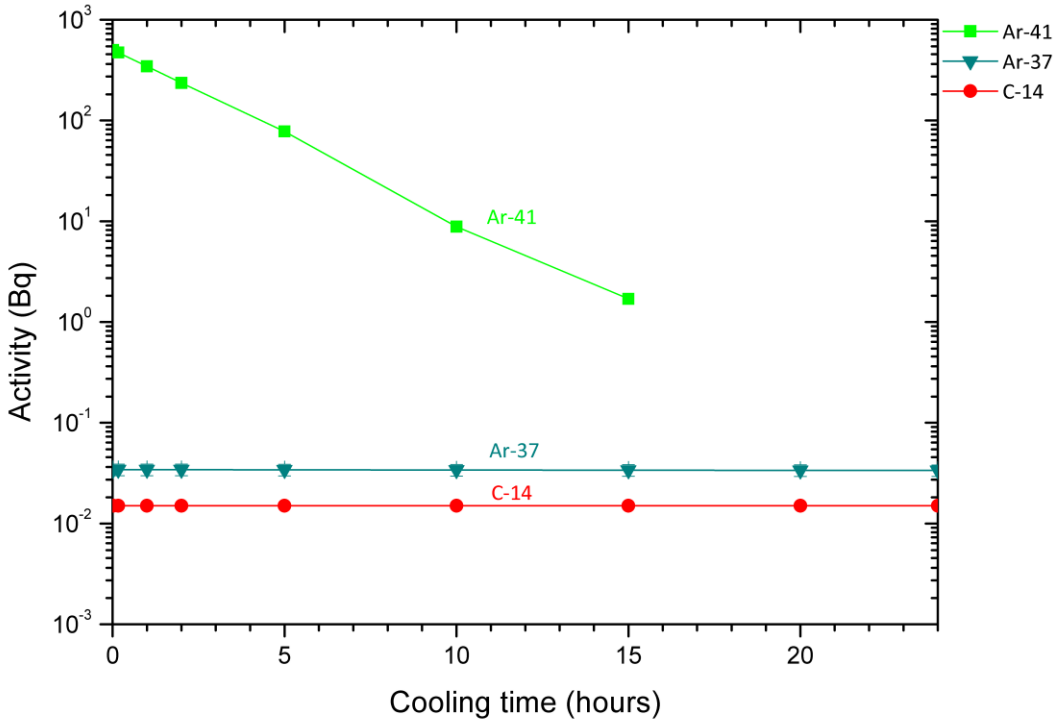

Fig.6. Activity of dominant radionuclides in air 0-24 hours after the end of activation with 2.45 MeV neutron source (fusion power: 2.68 MW; time of irradiation: 3000 s). Data shown only when the number of atoms is greater than $1 \cdot 10^4$.

Figs. 7 – 10 and Tabs. 3 – 6 show the evolution of specific activity and activity (given with uncertainty E) of the dominant radionuclides in air with time after EOI for 14 MeV neutron source (fusion power: 500 MW). The comparatively short radionuclide inventory for 1 g of air is because only those radionuclides that have minimum number of atoms greater than $1 \cdot 10^4$ were included.

In the case of the 14 MeV neutron source, the list of produced isotopes is longer in comparison to the neutron source of 2.45 MeV. It covers short-lived radionuclides such as N-13 ($T_{1/2}$ = 9.965 min), N-16 ($T_{1/2}$ = 7.13 s), Ar-41, Cl-38 ($T_{1/2}$ = 37.24 min), Cl-39 ($T_{1/2}$ = 55.6 min), Cl-40 ($T_{1/2}$ = 1.35 min), S-37 ($T_{1/2}$ = 5.05 min), Kr-83m ($T_{1/2}$ = 1.83 h), Kr-85m ($T_{1/2}$ = 4.48 h) and long-lived radionuclides such as Ar-37, Ar-39 ($T_{1/2}$ = 269 y), H-3 ($T_{1/2}$ = 12.33 y), C-14 and S-35 ($T_{1/2}$ = 87.32 d). These radionuclides would be of most concern for accidental release.

The pathway analysis was performed to list all the significant reaction channels (with their percentage contributions) leading to the production of a particular radionuclide following the irradiation of a target nuclide with 2.45 MeV and 14 MeV neutron sources. The results are presented in Tables 7 ÷ 9. Uncertainty estimates of the calculated activities were made by combining the pathway information with uncertainty data for cross sections.

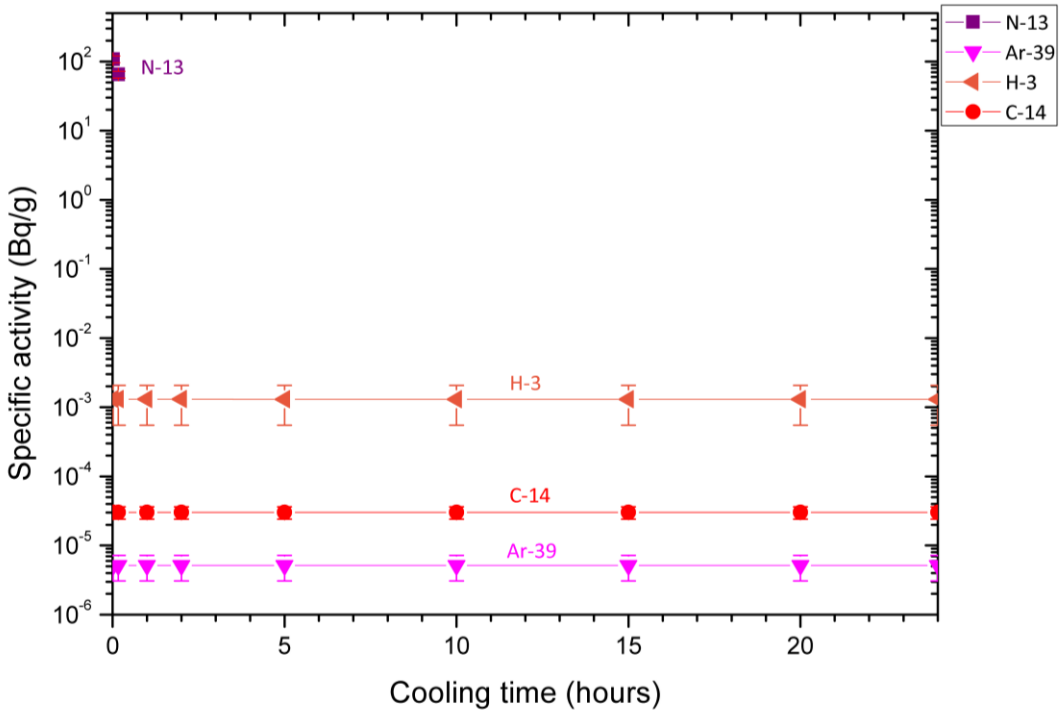

Fig.7. Specific activity of the dominant radionuclides in air 0-24 hours after the end of activation with 14 MeV neutron source (fusion power: 500 MW; time of irradiation: 400 s). Data shown only when the number of atoms is greater than $1 \cdot 10^4$.

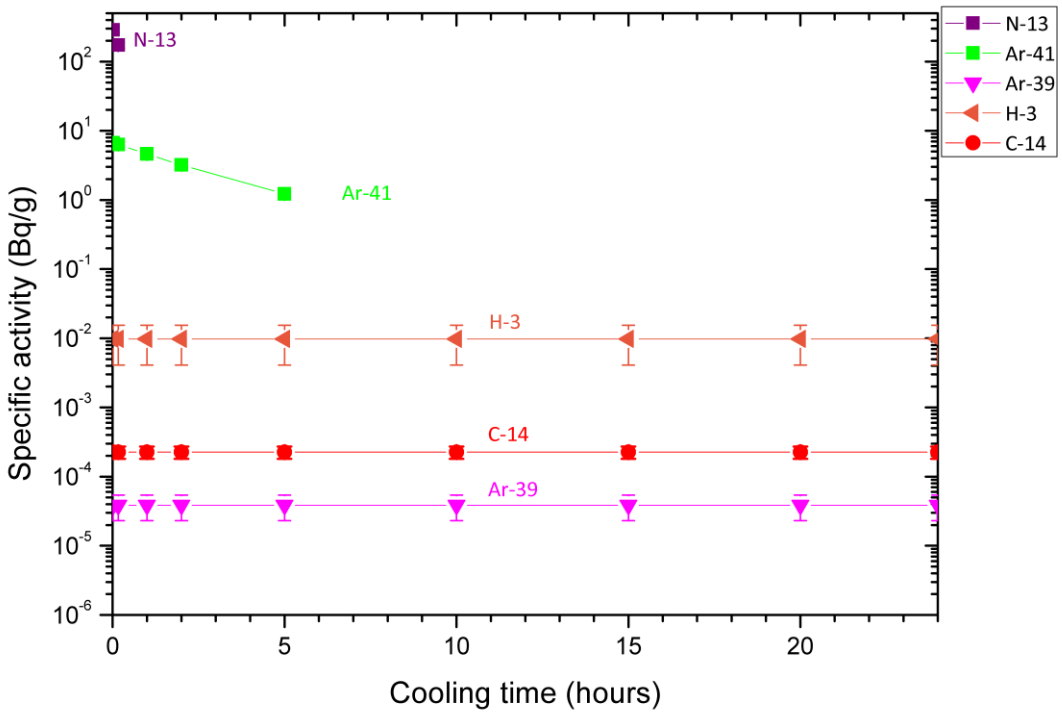

Fig.8. Specific activity of dominant radionuclides in air 0-24 hours after the end of activation with 14 MeV neutron source (fusion power: 500 MW; time of irradiation: 3000 s). Data shown only when the number of atoms is greater than $1 \cdot 10^4$.

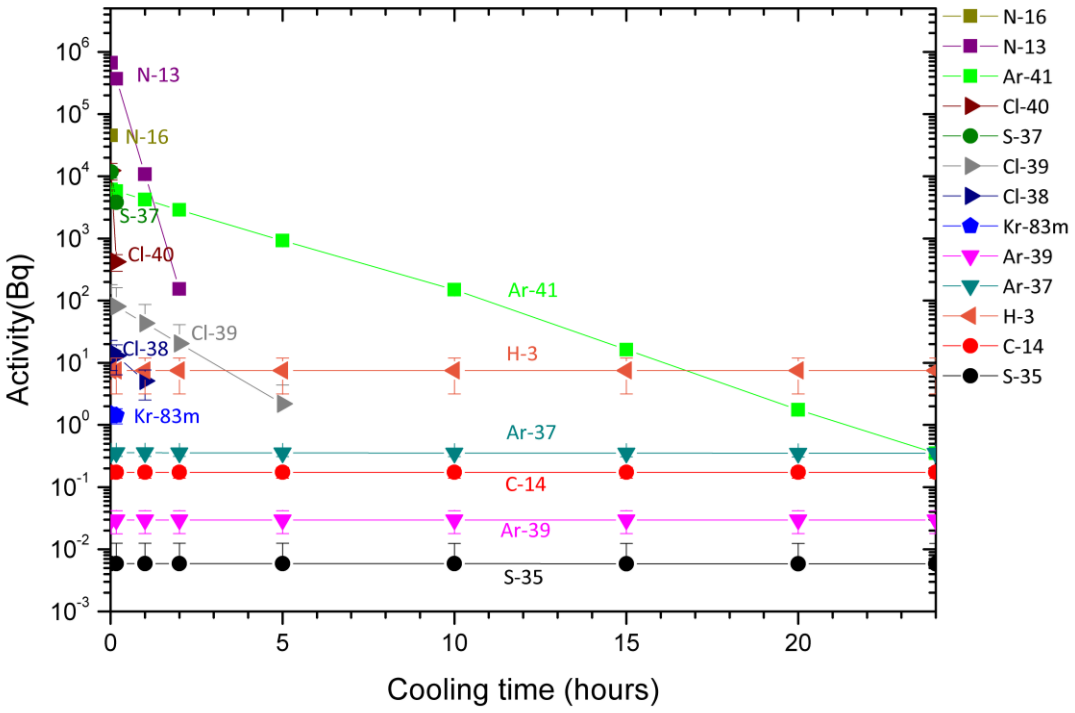

Fig.9. Activity of dominant radionuclides in air 0-24 hours after the end of activation with 14 MeV neutron source (fusion power: 500 MW; time of irradiation: 400 s). Data shown only when the number of atoms is greater than $1 \cdot 10^4$.

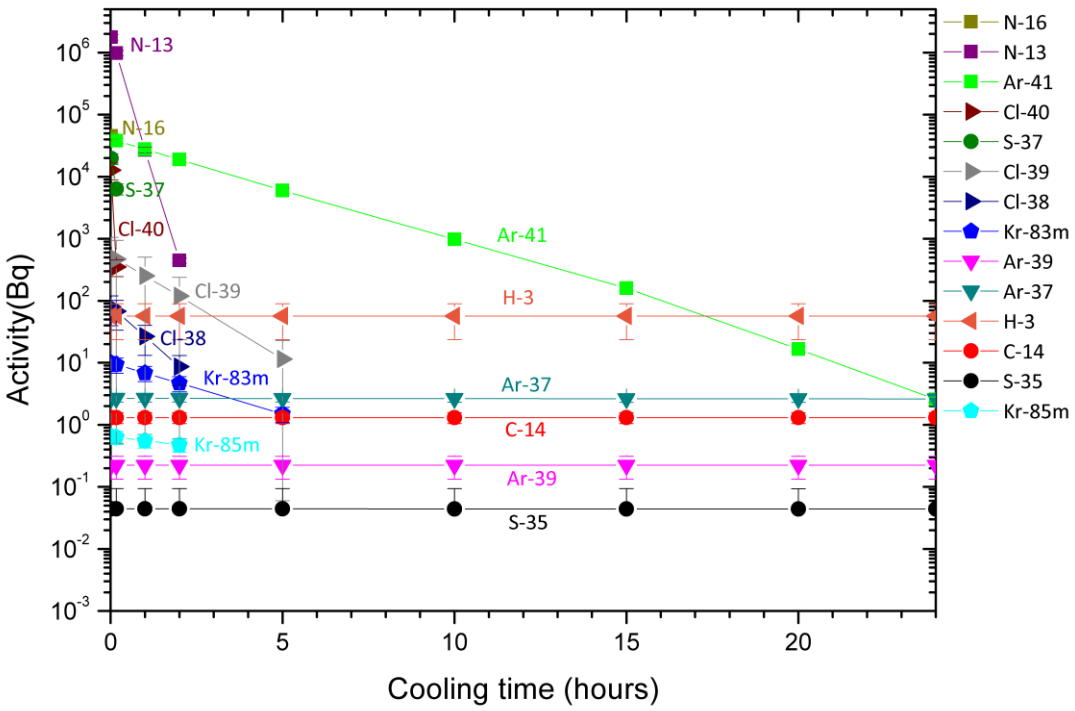

Fig.10. Activity of dominant radionuclides in air 0-24 hours after the end of activation with 14 MeV neutron source (fusion power: 500 MW; time of irradiation: 3000 s). Data shown only when the number of atoms is greater than $1 \cdot 10^4$.

Table 3. Specific activities of dominant radionuclides in air 0-24 hours after the end of activation (14 MeV neutron source, 1 g of air, t_{irr}=400 s).

	t = 1 min		*t = 10 min*		*t = 1 h*		*t = 10 h*		*t = 24 h*	
Nuclide	**Specific activity [Bq/g]**	**E(Specific activity) [Bq/g]**	**Specific activity [Bq/g]**	**E(Specific activity) [Bq/g]**	**Specific activity [Bq/g]**	**E(Specific activity) [Bq/g]**	**Specific activity [Bq/g]**	**E(Specific activity) [Bq/g]**	**Specific activity [Bq/g]**	**E(Specific activity) [Bq/g]**
N-13	1.081E+02	1.18E+01	6.501E+01	7.09E+00						
H-3	1.306E-03	7.58E-04	1.306E-03	7.58E-04	1.306E-03	7.58E-04	1.305E-03	7.58E-04	1.305E-03	7.58E-04
Ar-39	5.140E-06	2.06E-06	5.140E-06	2.06E-06	5.143E-06	2.06E-06	5.146E-06	2.06E-06	5.146E-06	2.06E-06
C-14	3.009E-05	6.01E-06	3.009E-05	6.01E-06	3.009E-05	6.01E-06	3.009E-05	6.01E-06	3.009E-05	6.01E-06
A_{total}=	**1.08E+05**	**1.18E+04**	**6.50E+04**	**7.09E+03**	**1.34E+00**	**7.58E-01**	**1.34E+00**	**7.58E-01**	**1.34E+00**	**7.58E-01**

A_{total} – *total activity [Bq]*; t_{irr} – *time of irradiation (duration of a discharge)*

Table 4. Specific activities of dominant radionuclides in air 0-24 hours after the end of activation (14 MeV neutron source, 1 g of air, t_{irr}=3000 s).

	t = 1 min		*t = 10 min*		*t = 1 h*		*t = 10 h*		*t = 24 h*	
Nuclide	**Specific activity [Bq/g]**	**E(Specific activity) [Bq/g]**	**Specific activity [Bq/g]**	**E(Specific activity) [Bq/g]**	**Specific activity [Bq/g]**	**E(Specific activity) [Bq/g]**	**Specific activity [Bq/g]**	**E(Specific activity) [Bq/g]**	**Specific activity [Bq/g]**	**E(Specific activity) [Bq/g]**
N-13	2.879E+02	3.01E+01	1.732E+02	1.81E+01						
Ar-41	6.675E+00	6.89E-01	6.314E+00	6.51E-01	4.629E+00	4.78E-01				
H-3	9.792E-03	5.68E-03	9.792E-03	5.68E-03	9.791E-03	5.68E-03	9.791E-03	5.68E-03	9.790E-03	5.68E-03
Ar-39	3.856E-05	1.54E-05	3.856E-05	1.54E-05	3.858E-05	1.54E-05	3.859E-05	1.54E-05	3.859E-05	1.54E-05
C-14	2.257E-04	4.51E-05	2.257E-04	4.51E-05	2.257E-04	4.51E-05	2.257E-04	4.51E-05	2.257E-04	4.51E-05
A_{total}=	**2.95E+05**	**3.01E+04**	**1.80E+05**	**1.81E+04**	**4.64E+03**	**4.78E+02**	**1.01E+01**	**5.68E+00**	**1.01E+01**	**5.68E+00**

Table 5. Activities of the dominant radionuclides in air 0-24 hours after the end of activation (14 MeV neutron source, air mass m=5.74 kg, t_{irr}=400 s).

	t = 1 min		*t = 10 min*		*t = 1 h*		*t = 10 h*		*t = 24 h*	
Nuclide	**Activity[Bq]**	**E(Activity) [Bq]**	**Activity[Bq]**	**E(Activity) [Bq]**	**Activity[Bq]**	**E(Activity) [Bq]**	**Activity[Bq]**	**E(Activity) [Bq]**	**Activity[Bq]**	**E(Activity) [Bq]**
N-16	4.54E+04	4.54E+03								
N-13	6.67E+05	6.73E+04	3.70E+05	3.73E+04	1.08E+04	1.09E+03				
Cl-40	1.24E+04	3.69E+03	4.21E+02	1.26E+02						
Ar-41	6.10E+03	5.99E+02	5.76E+03	5.66E+02	4.20E+03	4.13E+02	1.49E+02	1.47E+01		
S-37	1.17E+04	2.36E+03	3.81E+03	7.71E+02						
Cl-39	9.03E+01	9.05E+01	8.08E+01	8.10E+01	4.33E+01	4.34E+01				
Cl-38	1.53E+01	7.77E+00	1.30E+01	6.59E+00	5.10E+00	2.59E+00				
Kr-83m	1.51E+00	4.15E-01	1.43E+00	3.92E-01						
Ar-37	3.57E-01	4.57E-02	3.57E-01	4.57E-02	3.57E-01	4.57E-02	3.54E-01	4.54E-02	3.50E-01	4.48E-02
Ar-39	2.97E-02	1.19E-02	2.97E-02	1.19E-02	2.973E-02	1.19E-02	2.974E-02	1.19E-02	2.97E-02	1.19E-02
H-3	7.55E+00	4.38E+00	7.55E+00	4.38E+00	7.546E+00	4.38E+00	7.546E+00	4.38E+00	7.55E+00	4.38E+00
C-14	1.74E-01	3.48E-02	1.74E-01	3.48E-02	1.74E-01	3.48E-02	1.74E-01	3.48E-02	1.74E-01	3.48E-02
S-35	5.90E-03	6.63E-03	5.90E-03	6.63E-03	5.90E-03	6.63E-03	5.88E-03	6.61E-03	5.85E-03	6.57E-03
A_{total}=	**1.28E+05**	**1.17E+04**	**6.57E+04**	**6.46E+03**	**2.60E+03**	**2.02E+02**	**2.72E+01**	**2.65E+00**	**1.40E+00**	**7.58E-01**

A_{total} ***– total activity [Bq]*****; t_{irr}** ***– time of irradiation (duration of a discharge)***

Table 6. Activities of the dominant radionuclides in air 0-24 hours after the end of activation (14 MeV neutron source, air mass m=5.74 kg, t_{irr}=3000 s).

	t = 1 min		*t = 10 min*		*t = 1 h*		*t = 10 h*		*t = 24 h*	
Nuclide	**Activity[Bq]**	**E(Activity) [Bq]**	**Activity[Bq]**	**E(Activity) [Bq]**	**Activity[Bq]**	**E(Activity) [Bq]**	**Activity[Bq]**	**E(Activity) [Bq]**	**Activity[Bq]**	**E(Activity) [Bq]**
N-16	4.54E+04	4.54E+03								
N-13	1.78E+06	1.76E+05	9.83E+05	9.74E+04	2.70E+04	2.68E+03				
Ar-41	4.01E+04	3.93E+03	3.79E+04	3.72E+03	2.76E+04	2.71E+03	9.74E+02	9.56E+01	2.57E+00	2.52E-01
Cl-40	1.27E+04	3.82E+03	3.51E+02	1.05E+02						
S-37	1.96E+04	3.91E+03	6.36E+03	1.27E+03						
Cl-39	5.27E+02	5.26E+02	4.72E+02	4.71E+02	2.53E+02	2.52E+02				
Cl-38	7.98E+01	4.03E+01	6.76E+01	3.42E+01	2.66E+01	1.34E+01				
Kr-85m	6.47E-01	1.54E-01	6.32E-01	1.51E-01	5.56E-01	1.33E-01				
Kr-83m	9.93E+00	2.72E+00	9.39E+00	2.58E+00	6.85E+00	1.88E+00				
Ar-37	2.68E+00	3.43E-01	2.67E+00	3.43E-01	2.67E+00	3.43E-01	2.65E+00	3.40E-01	2.62E+00	3.36E-01
Ar-39	2.23E-01	8.91E-02	2.23E-01	8.91E-02	2.23E-01	8.92E-02	2.23E-01	8.92E-02	2.23E-01	8.92E-02
H-3	5.66E+01	3.29E+01	5.66E+01	3.29E+01	5.66E+01	3.29E+01	5.66E+01	3.29E+01	5.66E+01	3.29E+01
C-14	1.30E+00	2.61E-01	1.30E+00	2.61E-01	1.30E+00	2.61E-01	1.30E+00	2.61E-01	1.30E+00	2.61E-01
S-35	4.425E-02	4.97E-02	4.42E-02	4.97E-02	4.42E-02	4.97E-02	4.41E-02	4.95E-02	4.39E-02	4.93E-02
A_{total}=	**3.28E+05**	**3.05E+04**	**1.78E+05**	**1.69E+04**	**9.51E+03**	**6.60E+02**	**1.79E+02**	**1.75E+01**	**1.10E+01**	**5.68E+00**

A_{total} – ***total activity [Bq]***; **t_{irr}** – ***time of irradiation (duration of a discharge)***

PATHWAY ANALYSIS:

Symbols used in Tables 7 - 9: $T_{1/2}$ – half-life of radionuclide, IT – Internal transition.

Table 7. Results of pathway analysis for 2.45 MeV neutron source and 5.780385 kg of air

Nuclide	$T_{1/2}$	Reaction channel	Contribution [%]
Ar-41	109.34 min	Ar-40(n,γ)Ar-41	100
C-14	5730 y	N-14(n,p)C-14	100
Ar-37	35.04 d	Ar-36(n,γ)Ar-37	100

Table 8. Results of pathway analysis for 14 MeV neutron source and 1 g of air

Nuclide	$T_{1/2}$	Reaction channel	Contribution [%]
N-13	9,965 min	N-14(n,2n)N-13	100
Ar-41	109.34 min	Ar-40(n,γ)Ar-41	100
Ar-39	269 y	Ar-40(n,2n)Ar-39	99.95
H-3	12,33 y	N-14(n,t)H-3	99.82
C-14	5730 y	N-14(n,p)C-14	99.91

Table 9. Results of pathway analysis for 14 MeV neutron source and 5.780385 kg of air.

Nuclide	$T_{1/2}$	Reaction channel	Contribution [%]
N-16	7.13 s	O-16(n,p)N-16	99.999
N-13	9.965 min	N-14(n,2n)N-13	99.075
Cl-40	1.35 min	Ar-40(n,p)Cl-40	99.988
Ar-41	109.34 min	Ar-40(n,γ)Ar-41	99.972
S-37	5.05 min	Ar-40(n,α)S-37	98.620
Cl-39	55.6 min	Ar-40(n,np)Cl-39 Ar-40(n,d)Cl-39	1.95 98.05
Cl-38	37.24 min	Ar-38(n,p)Cl-38 Ar-38(n,p)Cl-38m---(IT)---Cl-38 Ar-40(n,t)Cl-38	48.755 50.283 0.669
Kr-85m	4.48 h	Kr-86(n,2n)Kr-85m Kr-84(n,γ)Kr-85m	74.456 25.598
Kr-83m	1.83 h	Kr-82(n,γ)Kr-83m Kr-83(n,n)Kr-83m Kr-84(n,2n)Kr-83m	64.193 4.193 31.561
Ar-39	269 y	Ar-40(n,2n)Ar-39	99.955
Ar-37	35.04 d	Ar-36(n,γ)Ar-37 Ar-38(n,2n)Ar-37	96.605 3.395
H-3	12.33 y	N-14(n,t)H-3	99.817
C-14	5730 y	N-14(n,p)C-14	99.908
S-35	87.32 d	Ar-36(n,2p)S-35 Ar-38(n,α)S-35	54.475 45.525

Fig. 11 presents the total activity of the dominant radionuclides produced in air following the irradiation with 14 MeV neutron source (fusion power: 500 MW) at 0-24 h after EOI.

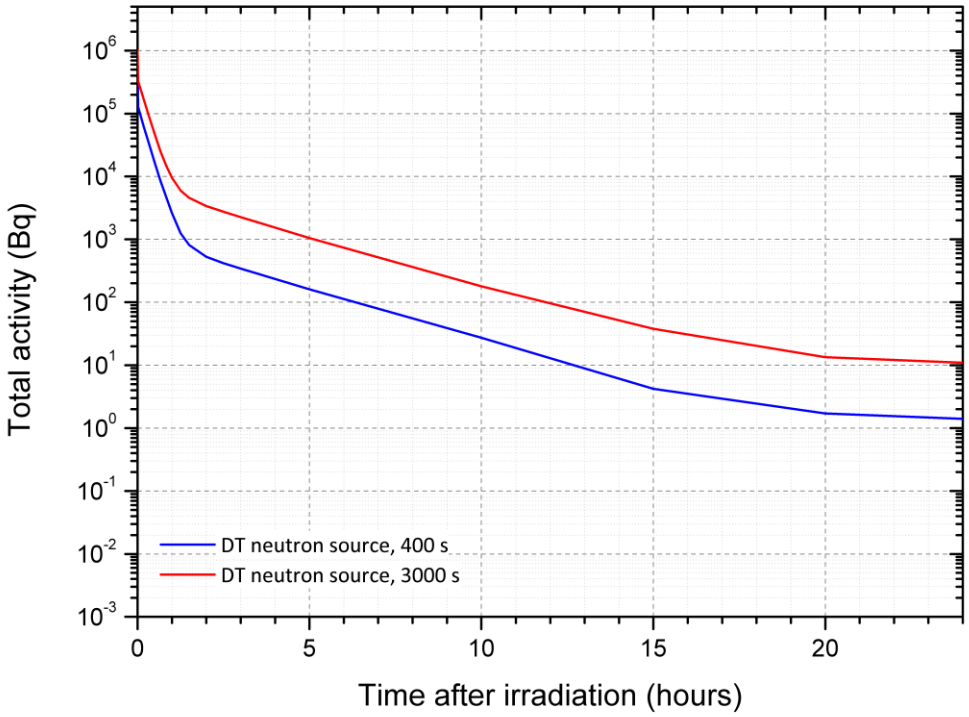

Fig. 11. Total activity of dominant radionuclides produced in air following the irradiation with 14 MeV neutron source (fusion power: 500 MW, t_{irr} = 400 s and 3000s).

In order to estimate if the obtained activities are not too high, especially from the radiological protection point of view, the calculated activities were compared with the ones defined as a maximum permissible by the regulations of the International Commission on Radiological Protection (ICRP). The ICRP established two basic concepts which are used in monitoring the activities of radionuclides in air. The first one is the Annual Limits of Intake (ALI), the second is the Derived Air Concentrations (DAC). ALI is a derived limit for the amount of radioactive material taken into the body of an adult worker by inhalation (or ingestion) in one year. ALI is the smaller value of intake of a given radionuclide in one year by the "reference man" that would result in the committed effective dose equivalent (CEDE) of 0.05 Sievert or the committed dose equivalent (CDE) of 0.5 Sievert to any individual organ or tissue. DAC is the average atmospheric concentration of the radionuclide which would lead to ALI in a reference person as a consequence of exposure at DAC for the 2000 hour working year. It is assumed that the reference person inhales 20 litres of air per minute or 2400 m^3 during the working year (under working conditions of "light work") [10].

The ALI and DAC values recommended by the ICRP for the radionuclides present in the irradiated air are shown in Table 10 [11].

Table 10. Annual Limits of Intake (ALI) and Derived Air Concentrations (DAC) - derived limits intended to control chronic occupational exposures (Table based on values recommended by the International Commission on Radiological Protection (ICRP)) [11].

Element (atomic number)	Radionuclide	ALI (Bq) / DAC in air (Bq/m^3) [over a year]
Argon (18)	Ar-37	- / $3.7 \cdot 10^{10}$
	Ar-39	- / $7.4 \cdot 10^{6}$
	Ar-41	- / $1.11 \cdot 10^{5}$
Carbon (6)	C-14	$7.4 \cdot 10^{10}$ / $2.59 \cdot 10^{7}$
Chlorine (17)	Cl-38	$1.48 \cdot 10^{9}$ / $7.4 \cdot 10^{5}$
	Cl-39	$1.85 \cdot 10^{9}$ / $7.4 \cdot 10^{5}$
Hydrogen (1)	H-3	$2.96 \cdot 10^{9}$ / $7.4 \cdot 10^{5}$
Krypton (36)	Kr-83m	- /$3.7 \cdot 10^{8}$
	Kr-85m	- /$7.4 \cdot 10^{5}$
	Kr-85	- /$3.7 \cdot 10^{6}$
Nitrogen (7)	N-13	- / $1.48 \cdot 10^{5}$
Sulphur (16)	S-35	$3.7 \cdot 10^{8}$ / $2.22 \cdot 10^{5}$
Phosphorus (15)	P-32	$3.33 \cdot 10^{7}$ / $1.48 \cdot 10^{4}$

To be able to compare the recommended DAC values with the one expected for the HRNS cuboid, the following scenario was considered:

- during the one day of ITER DT operation twenty discharges – each lasting 400 s – come one after another; the delay between the discharges is 3920 s;
- the fusion power is 500 MW except for the last three discharges for which it is 700 MW (as assumed in SA2 – 'safety operating scenario' – for the final day of DT operation) [7],
- the walls of the cuboid are 100% airtight so no air leakage or air exchange is possible;
- the concentrations of the dominant radionuclides in air are determined at 10 min, 30 min, 1h, 5 h and 8 h after the end of the last discharge.

The results of FISPACT calculations are presented in Table 11. It is clearly seen that even if the minimum time between the end of one discharge and the beginning of the next discharge at ITER would be on the level of about 3920 s, there is no possibility that the concentration of any radionuclides will exceed the DAC values, much less that in the real conditions:

- the air leakage for the port cells is expected on the level of 100% of the volume per day [12],
- the air in the tokamak galleries and vault will be exchanged once an hour [12].

Such the air exchange rate in the tokamak building is in accordance with the ISO standard 17873. This standard imposes also some requirements on the pressure hierarchy in the tokamak building that ensures a directed airflow from low level contamination towards high level contamination areas (i.e.

Table 11. Concentrations of the dominant radionuclides in air at 10 min, 30 min, 1 h, 5 h and 8 h after the end of series of twenty ITER discharges (14 MeV neutron source, air mass m= 5.74 kg, air volume V = 4.80 m^3).

	t = 10 min		*t = 30 min*		*t = 1 h*		*t = 5 h*		*t = 8 h*	
Nuclide	**Concentration [Bq/m^3]**	**Error [Bq/m^3]**	**Concentration [Bq/m^3]**	**Error [Bq/m^3]**	**Concentration [Bq/m^3]**	**Error [Bq/m^3]**	**Concentration [Bq/m^3]**	**Error [Bq/m^3]**	**Concentration [Bq/m^3]**	**Error [Bq/m^3]**
Ar-41	2.68E+03	2.63E+02	2.36E+03	2.31E+02	1.95E+03	1.91E+02	4.40E+02	4.31E+01	1.45E+02	1.42E+01
N-13	1.36E+03	1.11E+02	3.41E+02	2.79E+01	4.26E+01	3.48E+00				
Cl-39	1.68E+01	1.65E+01	1.31E+01	1.28E+01	8.99E+00	8.83E+00	5.83E-01	5.73E-01		
Cl-38	1.49E+00	6.96E-01	1.03E+00	4.79E-01						
H-3	3.09E+01	1.79E+01	3.09E+01	1.79E+01	3.09E+01	1.79E+01	3.09E+01	1.79E+01	3.09E+01	1.79E+01
Ar-39	1.22E-01	4.85E-02	1.22E-01	4.85E-02	1.22E-01	4.85E-02	1.22E-01	4.85E-02	1.22E-01	4.85E-02
Ar-37	1.45E+00	1.85E-01	1.45E+00	1.85E-01	1.45E+00	1.85E-01	1.44E+00	1.85E-01	1.44E+00	1.84E-01
C-14	7.12E-01	1.42E-01	7.12E-01	1.42E-01	7.12E-01	1.42E-01	7.12E-01	1.42E-01	7.12E-01	1.42E-01
Kr-85m	1.01E-01	2.56E-02	9.55E-02	2.42E-02						
Kr-83m	6.67E-01	1.86E-01	5.88E-01	1.64E-01	4.87E-01	1.36E-01				
Kr-85	4.81E-05	1.33E-05	4.82E-05	1.33E-05	4.83E-05	1.33E-05	4.87E-05	1.34E-05	4.89E-05	1.35E-05
S-35	2.41E-02	2.71E-02	2.41E-02	2.71E-02	2.41E-02	2.71E-02	2.40E-02	2.71E-02	2.40E-02	2.69E-02
P-32	3.24E-03	6.48E-03	3.24E-03	6.48E-03	3.24E-03	6.48E-03	3.21E-03	6.42E-03	3.19E-03	6.38E-03

to the inside of the building). In result, the port cells, located in so called yellow zones of the tokamak complex, will be kept at a sub-atmospheric pressure of -100 Pa [12]. With such pressure, the density of air (at the temperature T= 295.15 K) is equal to 1.19 $kg \cdot m^{-3}$, so the mass of air in the cuboid m = 5.73 kg. Therefore, the expected concentrations of the radioactivities will be slightly lower than the ones already calculated.

Although none of the ITER port cells is connected to the ventilation and air conditioning systems (HVAC), at normal conditions they are connected to the detritiation system (DS) via dedicated air ducts. If a tritium release enhances, the air flow rate for a port cell will be automatically enlarged (by opening corresponding isolation valves) [12]. From among all the radionuclides produced in air, tritium is of the most concern. The tritium concentration in the air is monitored by on line tritium monitors. During the DT operations H-3 will be produced in air via the N-14(n,t)H-3 reaction. H-3 decays with the half-life of 12.33 years by beta decay into a He-3 isotope. The mean kinetic energy release in the β-electron is ≈ 5.6 keV, the maximum at 18.59 keV. With the assumed irradiation scenario the calculated concentration of activity of H-3 in the cuboid for the 14 MeV neutron source is equal to (3.09E+01 ± 1.79E+01) Bq/m^3. Such concentration is seven orders of magnitude lower than the predetermined action limit for tritium concentration in room air that is equal to $1 \cdot 10^8$ Bq/m^3.

Conclusions

The production of radionuclides in air inside the second Cuboid of the HRNS system in the ITER equatorial port cell #1 has been investigated. The results show that a single DD or DT tokamak discharge would generate small amounts of air activation. This activation will not be significant even in routine tokamak operations when at least several discharges are foreseen per day. The concentrations of long-lived radionuclides which are of most concern, e.g. C-14, Ar-37 (for DD and DT plasma operations) or H-3, Ar-39 (for DT plasma operation), will not exceed the maximum permissible levels.

References

[1] L. Bertalot, 1 R. Barnsley, M.F. Direz, J.M. Drevon, A. Encheva, S. Jakhar, Y. Kashchuk, K.M. Patel, A.P. Arumugam, V. Udintsev, C. Walker, M. Walsh, Fusion neutron diagnostics on ITER tokamak, Journal of Instrumentation, Vol. 7 (2012)

[2] Technical specification for the conceptual design and interface specification of High Resolution Neutron Spectrometer, F4E_D_24GRTW v4.3

[3] F4E_D_23SFUK v.1.0, MEETING SUMMARY - F4E-GRT-403 / 2WM

[4] M. Scholz et al., System Design Description Document (DDD) High Resolution Neutron Spectrometer DDD-PBS 55.BB (Enabled), (2016) ITER_DDD 55.BB.HRNS v1.1

[5] X-5 Monte Carlo Team, MCNP – A General Monte Carlo N-Particle Transport Code Version 5 *Los Alamos National Laboratory* LA-UR-03-1987, (2008)

[6] M. Mazur, Systemy ochrony powietrza, Uczelniane Wydawnictwa Naukowo-Dydaktyczne AGH, (2004), Kraków, Poland

[7] M. Loughlin, N. Taylor, Recommendation on Plasma scenarios, (2009) ITER_2V3V8G v1.2.

[8] J.Ch. C. Sublet, J. W. Eastwood, J. G. Morgan, The FISPACT II user manual (2014) CCFE

[9] V.Chuyanov, Interface of Blanket Testing and ITER design, presentation (2014) http://fti.neep.wisc.edu/tofeprogram/oral/O-I-5.1.pdf

[10] A. A. Cigna, M. Durante, Radiation Risk Estimates in Normal and Emergency Situations, Springer Science & Business Media, (2007), Berlin, Germany

[11] Annual limits on intake (ALI) and derived air concentrations (DAC) of radionuclides for occupational exposure; effluent concentrations; concentrations for release to sanitary sewerage. http://www.nrc.gov/reading-rm/doc-collections/cfr/part020/appb/index.html#S

[12] D.Schlagheck, L. Lepetit, Design study of HVAC and tritium confinement systems in the ITER Tokamak Complex – Design Description Document (DDD) for the HVAC, Final report prepared to EFDA, (2008) ITER_D_2ERQH6 v1.0.

Appendix 1. Cross sections of the considered reactions taken from EAF-2010 nuclear data libraries.

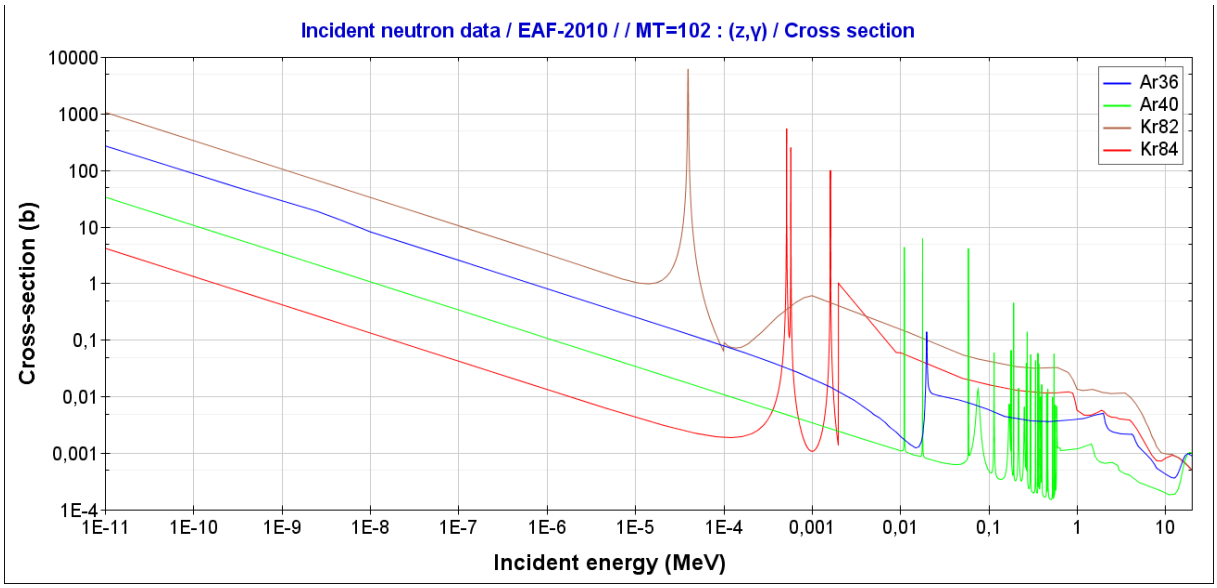

Fig.A1. Cross sections for (n,γ) reactions on Ar-36, Ar-40 Kr-82 and Kr-84.

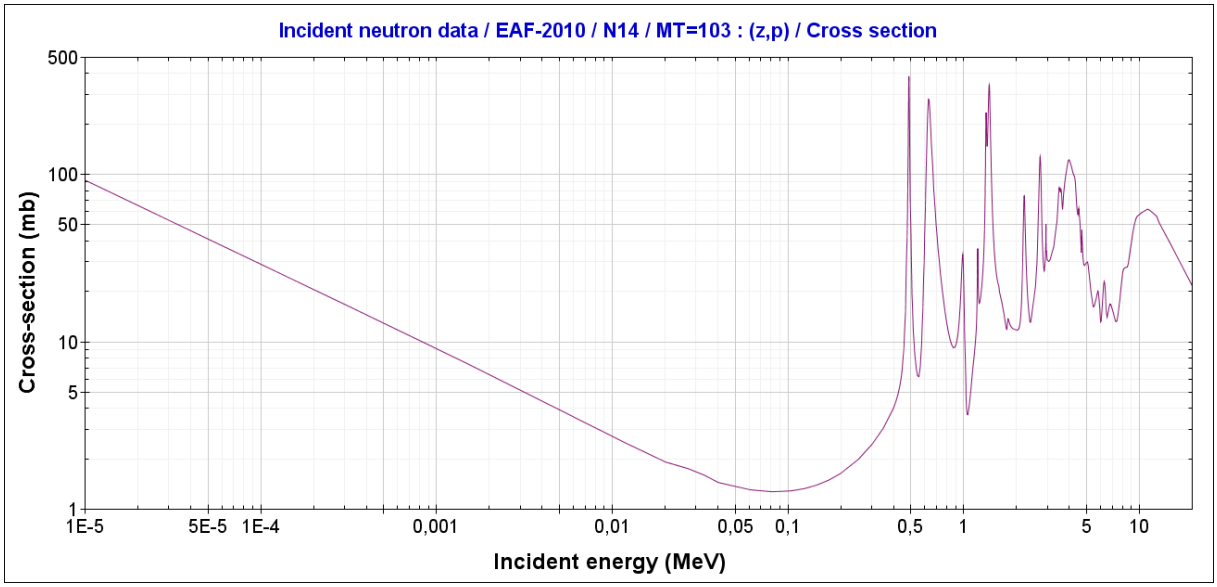

Fig.A2. Cross section for (n,t) reaction on N-14.

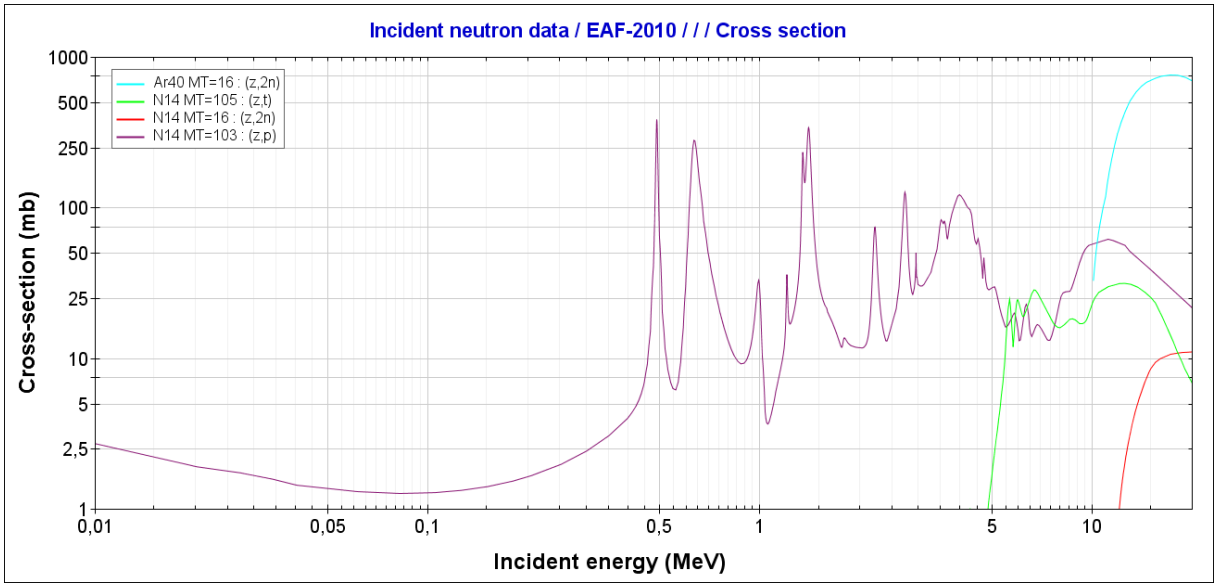

Fig.A3. Cross section for (n,2n) reactions on Ar-40 and (n,p), (n,2n) and (n,t) reactions on N-14.

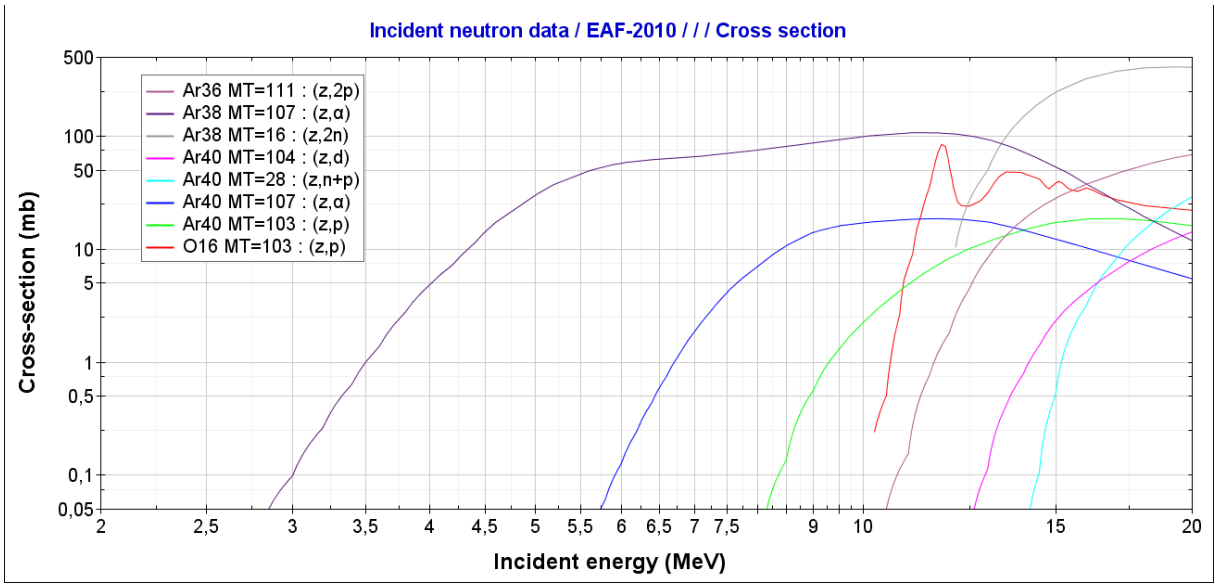

Fig.A4. Cross sections for (n,2p) reaction on Ar-36; (n,α) and (n, 2n) reactions on Ar-38; (n,d), (n,np) (n,α) and (n,p) reactions on Ar-40; and (n,p) reaction on O-16.